

Density Functional Theory Investigations on the Chemical Basis of the Selectivity Filter in the K⁺ Channel Protein

Fuqiang Ban,[†] Peter Kusalik,[†] and Donald F. Weaver^{*,†,‡,§}

Contribution from the Department of Chemistry, Department of Medicine, and School of Biomedical Engineering, Dalhousie University, Halifax, NS, Canada B3H 4J3

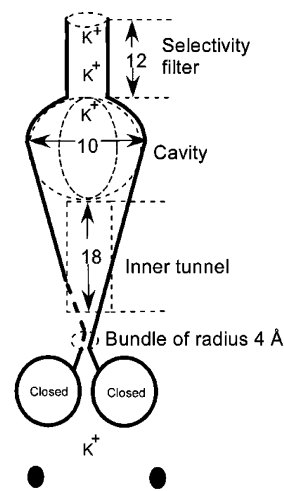
Received June 17, 2003; E-mail: donald.weaver@dal.ca

Abstract: The chemical–physical basis of loading and release of K⁺ and Na⁺ ions in and out of the selectivity filter of the K⁺ channel has been investigated using the B3LYP method of density functional theory. We have shown that the difference between binding free energies of K⁺ and Na⁺ to the cavity end of the filter is smaller than the difference between the K⁺ and Na⁺ solvation free energies. Thus, the loading of K⁺ ions into the cavity end of the selectivity filter from the solution phase is suggested to be selective prior to the subsequent conduction process. It is shown that the extracellular end of the filter is only optimal for K⁺ ions, because K⁺ ions prefer the coordination environment of eight carbonyl oxygens. Na⁺ ions do not fit into the extracellular end of the filter, since they prefer the coordination environment of six carbonyl oxygens. Overall, the results suggest that the rigid C₄ symmetric selectivity filter is specifically designed for conduction of K⁺ ions.

Introduction

The K⁺ channel shuttles K⁺ ions from intracellular to extracellular environments and is central to regulating many fundamental physiological functions, especially in the heart and brain. High selectivity and rapid transmission of K⁺ ions are the unique properties of K⁺ channels. Two fundamental questions persist in structural studies of transmembrane K⁺ channels: (1) What is the chemical basis by which the channel distinguishes between the featureless spheres of K⁺ and Na⁺, and (2) how can K⁺ channels be highly selective, yet allow K⁺ to diffuse through the channel rapidly?¹

The KcsA K⁺ channel protein crystal structure has been solved by Doyle et al.¹ The architecture of the KcsA K⁺ channel is schematically shown in Figure 1. It is composed of three parts that include an “inner tunnel” of 18 Å from the inner surface of the cell, a “cavity” of diameter of approximately 10 Å in the middle of the membrane, and a narrow 12 Å “selectivity filter” leading outside the cell. Jiang et al. analyzed the conformational difference between the “opened state” and “closed state” of the KcsA and MthK channels.^{2,3} The crystal structure of the truncated KcsA K⁺ channel corresponds to a closed state in which the four inner α-helices form a right-handed bundle at an entrance pore of radius 4 Å near the intracellular opening.² The crystallographic study of Zhou et al. suggested that the intracellular half of the pore can open to a distance of 10 Å.⁴



Regulators of K⁺ Conductance

Figure 1. Schematic representation of the KcsA K⁺ channel.

Their studies inferred that the inner half of the KcsA K⁺ channel is more dynamically sensitive and is responsible for the gating that controls the diffusion of the K⁺ ion into the cavity. The desired K⁺ ion concentration within cells is maintained by the equilibrium of K⁺ outflow and influx (see Figure 2).

MacKinnon and co-workers⁵ have confirmed that two glycine residues (positions 1 and 3 in Figure 3) in the selectivity filter are strictly conserved over many types of K⁺ channels, and the variation of residues at positions 2, 4, and 5 is only restricted to between tyrosine and phenylalanine, valine and isoleucine,

[†] Department of Chemistry.

[‡] Department of Medicine.

[§] School of Biomedical Engineering.

- (1) Doyle, D. A.; Cabral, J. M.; Pfuetzner, R. A.; Kuo, A. L.; Gulbis, J. M.; Cohen, S. L.; Chait, B. T.; MacKinnon, R. *Science* **1998**, *280*, 69.
- (2) Jiang, Y. X.; Lee, A.; Chen, J. Y.; Cadene, M.; Chait, B. T.; MacKinnon, R. *Nature* **2002**, *417*, 523.
- (3) Jiang, Y. X.; Lee, A.; Chen, J. Y.; Cadene, M.; Chait, B. T.; MacKinnon, R. *Nature* **2002**, *417*, 515.

(4) Zhou, M.; Morais-Cabral, J. H.; Mann, S.; MacKinnon, R. *Nature* **2001**, *411*, 657.

(5) MacKinnon, R.; Cohen, S. L.; Kuo, A. L.; Lee, A.; Chait, B. T. *Science* **1998**, *280*, 106.

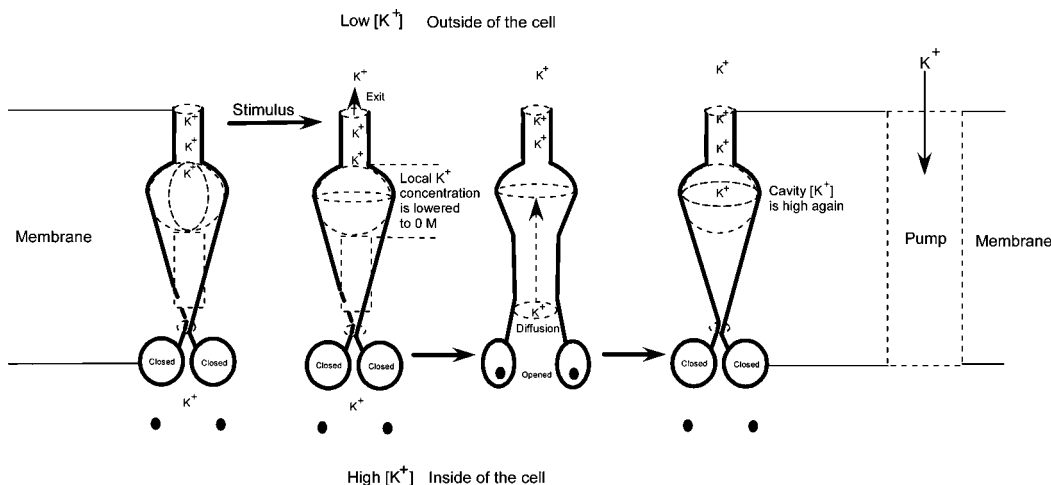


Figure 2. Schematic illustration of the outflow and influx of K^+ ions across the cellular membrane.

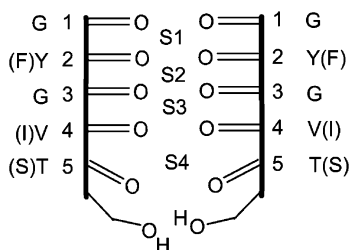


Figure 3. Schematic illustration of the selectivity filter.

and threonine and serine, respectively. The side chains of each of these three pairs of amino acids possess a unique similarity: a β -OH group characterizes threonine and serine side chains, a tertiary β -carbon characterizes valine and isoleucine side chains, and a α -phenyl group characterizes tyrosine and phenylalanine side chains. The unique properties of these three pairs of amino acids and glycine combine to construct the selectivity filter within the K^+ channel protein. Maser et al. reported that glycine residues in potassium channel-like selectivity filters determine potassium selectivity.⁶ However, the chemical–physical basis for the unique combination of these amino acids to form the filter has not been elucidated.

The molecular environment of the selectivity filter is further characterized by four “binding sites” (S1 to S4, extracellular to intracellular; Figure 3), which is formed by the oxygen atoms of residues T(S)⁷⁵-V(I)⁷⁶-G⁷⁷-Y(F)⁷⁸-G⁷⁹. Since the amino acid sequences of the selectivity filters of various species are highly conserved,¹ the selectivity filter is considered to be the central element of K^+ channels. Within the KcsA K^+ channel, multiple K^+ ions exist in its conduction pore. In the closed state, one K^+ ion sits in the cavity that is filled with water, while the other two K^+ ions reside in the narrow selectivity filter. It is postulated that the K^+ selectivity filter catalyzes the dehydration, transfer, and rehydration of a K^+ in approximately 10 ns.

Molecular dynamic simulations by Aqvist and Luzhkov⁷ concluded that the occupation of the selectivity filter by two K^+ ions and two H_2O molecules is thermodynamically favored and that any conducting mechanism involving three K^+ ions in the filter can be excluded. The only function of the wide cavity

in the middle of the membrane was to help overcome the dielectric barrier of the membrane. Free energy calculations by Roux and MacKinnon⁸ showed that the transfer of a single K^+ ion from bulk water to the cavity center with two ions in the selectivity filter is favored by 8.5 kcal mol⁻¹ and that the KcsA cavity provides monocation selectivity over polyvalent cation. More recent molecular dynamic simulations by Berneche and Roux⁹ suggested that multiple pathways of the knock-on mechanism and the vacancy-diffusion mechanism are feasible for the rapid translocation of K^+ ions through the channel (in the configuration of (cavity)^{K+}(S4)^{H₂O}(S3)^{K+}(S2)^{H₂O}(S1)^{K+}). The largest free energy barrier for the knock-on mechanism was estimated to be 2–3 kcal/mol, while the barrier for the vacancy-diffusion mechanism was 3–4 kcal/mol. Moreover, since their calculations showed that the magnitude of the dynamic fluctuation is larger than the Pauling radius difference of 0.38 Å between Na^+ (0.95 Å) and K^+ (1.33 Å) ions, they concluded that selectivity does not arise only from simple geometric considerations.

More interestingly, it has been reported that K^+ channels exclude the smaller alkali metal cation Li^+ (radius, 0.6 Å) and Na^+ (0.95 Å) but allow permeation by the larger ions Rb^+ (1.48 Å) and Cs^+ (1.69 Å).¹ Luzhkov and Aqvist suggested that the most feasible mechanism for the K^+ translocation is the switch of two occupancy states of (S1)^{H₂O}(S2)^{K+}(S3)^{H₂O}(S4)^{K+} and (S1)^{K+}(S2)^{H₂O}(S3)^{K+}(S4)^{H₂O} in the selectivity filter. Their estimated activation barrier from (S1)^{H₂O}(S2)^{K+}(S3)^{H₂O}(S4)^{K+} to (S1)^{K+}(S2)^{H₂O}(S3)^{K+}(S4)^{H₂O} is 6 kcal mol⁻¹. For the same mechanisms, the activation barriers of Na^+ and Rb^+ ions are calculated to be 3.5 and 1.7 kcal mol⁻¹ higher than that of K^+ . The experiments of MacKinnon and co-workers support the above two-state switching mechanism as the most favored pathway for the permeation of K^+ and Rb^+ across the KcsA channel.¹⁰ Furthermore, their electron density analysis suggested that the KcsA filter is more energetically optimized for K^+ than Rb^+ . It has been suggested that the 10⁴ margin by which K^+ ions are selected over Na^+ implies stronger interactions between K^+ and the selectivity filter than those of Na^+ ions. The suggested strong interaction is obviously against the rapid movement of the K^+ through the pore.

(6) Maser, P.; Hosoo, Y.; Goshima, S.; Horie, T.; Eckelman, B.; Yamada, K.; Yoshida, K.; Bakker, E. P.; Shimmyo, A.; Oiki, S.; Schroeder, J. I.; Uozumi, N. *Proc. Natl. Acad. Sci. U.S.A.* **2002**, *99*, 6428.

(7) Aqvist, J.; Luzhkov, V. *Nature* **2000**, *404*, 881.

(8) Roux, B.; MacKinnon, R. *Science* **1999**, *285*, 100.

(9) Berneche, S.; Roux, B. *Nature* **2001**, *414*, 73.

(10) Morais-Cabral, J. H.; Zhou, Y. F.; MacKinnon, R. *Nature* **2001**, *414*, 37.

Zhou et al. observed that the eight waters of the inner hydration shell of the K⁺ in the cavity are ordered in a square antiprism, in which the K⁺ sits between two layers of four waters.¹¹ The layers of 4-fold carbonyl oxygens within the filter offer K⁺ a desired coordination environment to smoothly take the K⁺ ions from their 4-fold solvation structure within water.

Density functional calculations on models taken from selected snapshots of a molecular dynamics simulation suggested that the K⁺-induced polarization effects play a significant role in the microscopic mechanisms regulating potassium permeation.¹² Shrivastava et al.'s molecular dynamic (MD) simulations revealed significant differences in interactions of K⁺ and Na⁺ ions with the selectivity filter. In particular, their results suggested that K⁺ ions prefer an eight-coordination environment provided by the oxygens of the filter and Na⁺ ions prefer a six-coordination environment provided by four oxygens of the filter and two water molecules.¹³

In the present paper, the chemical–physical basis for the loading and release of K⁺ and Na⁺ ions in to and out of the selectivity filter of the K⁺ ion channel protein has been investigated using the B3LYP method of density functional theory.

Computational Methods

K⁺ ions can diffuse rapidly across the filter segment; Berneche and Roux's molecular dynamic simulations have shown that the activation free energy for the conduction of K⁺ along the filter is very small.⁹ Thus, we have simplified the filter as a cylinder whose two ends possess the same molecular structures as the real filter (see Figure 4). Although shuttling a K⁺ ion from one end to the other end of the filter has small barriers, the two ends of the cylinder are considered to be crucial to the control of the loading and release of K⁺ ions. The cavity and extracellular ends of the filter are modeled by the systems of A and B that are schematically shown in Figure 4. The initial geometries of A and B for geometry optimization were extracted from the known crystal structure of the KcsA K⁺ channel. Since there are approximately 50 molecules in the cavity, it is assumed that the K⁺ ion is essentially fully solvated as it is in bulk solution.

All geometry optimizations were performed with the B3LYP hybrid density functional in conjunction with the 6-31G(d) basis set using the GAUSSIAN 98 suite of programs.¹⁴ The B3LYP functional is a combination of Becke's three-parameter hybrid exchange functional,^{15,16} as implemented in GAUSSIAN 98,¹⁷ and the Lee–Yang–Parr correlation functional.¹⁸ Harmonic vibrational frequencies and zero-point vibrational energy (ZPVE) corrections were calculated at the same level of theory. Relative energies at 0 K were obtained by performing single

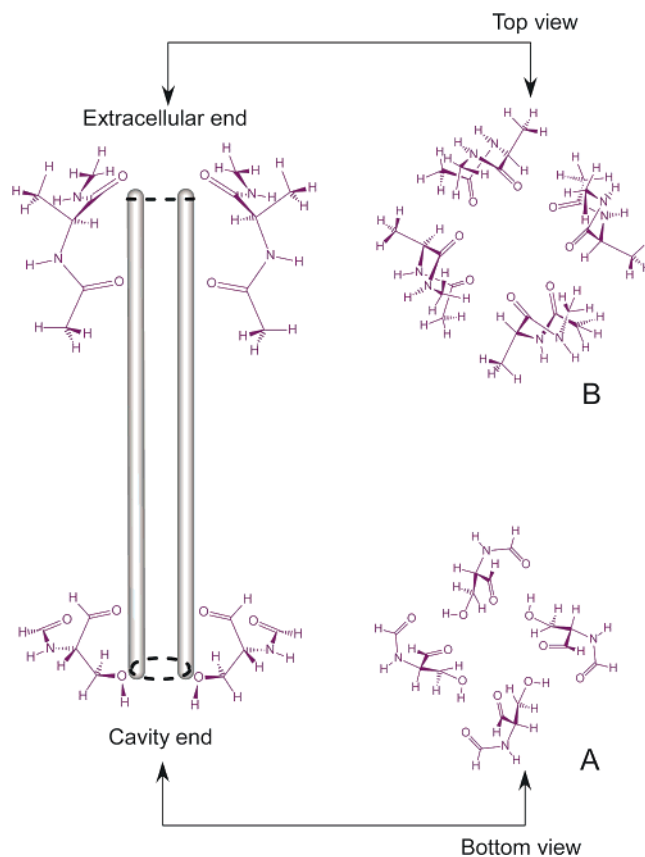


Figure 4. Schematic illustration of the model filter and the structures of A and B.

point calculations at the B3LYP level in conjunction with the 6-311+G(2df,p) basis set with use of the above optimized geometries and with inclusion of the ZPVE, i.e., B3LYP/6-311+G(2df,p)/B3LYP/6-31G(d) + ZPVE. Estimates for relative Gibbs free energies at the standard condition were obtained by performing single-point calculations at the B3LYP level in conjunction with the 6-311+G(2df,p) basis set with use of the above optimized geometries and with inclusion of thermal corrections of translational, rotational, and vibrational motions from B3LYP/6-31G(d) frequency calculations, i.e., B3LYP/6-311+G(2df,p)/B3LYP/6-31G(d) + thermal correction.

All energies are in kilocalories per mole, unless otherwise specified. The optimized structures of all species encountered in this present study are given in Table S1 of the Supporting Information.

Results and Discussion

Selectivity of the Cavity End. To elucidate how the filter may select K⁺ rather than Na⁺ at the cavity end, the loading of a K⁺ ion and a Na⁺ ion from the cavity into the filter is separated into two sequential steps, schematically shown in Figure 5. The first step is the dehydration of the solvated K⁺ and Na⁺ ions. We assumed that the solvation energies of K⁺ and Na⁺ ions in the cavity are approximately the same as solvation energies in bulk water. The second step is the coordination of the bare K⁺ and Na⁺ ions within the cavity end of the filter.

To examine the role of the K⁺ and Na⁺ affinities in selectivity, we first studied step 2 of our model in Figure 5. The optimized complexes (hereafter denoted as K⁺–A and Na⁺–A) are shown in Figure 6. For K⁺–A, the two layers of oxygen atoms that form a sandwich structure with the K⁺ ion assume a staggered conformation. The diameter (5.111 Å) of the first ring of OH oxygens on the cavity side is smaller than

- (11) Zhou, Y. F.; Morais-Cabral, J. H.; Kaufman, A.; MacKinnon, R. *Nature* **2001**, *414*, 43.
- (12) Guidoni, L.; Carloni, P. *Biochim. Biophys. Acta* **2002**, *1563*, 1.
- (13) Shrivastava, I. H.; Tieleman D. P.; Biggin, P. C.; Sansom, M. S. P. *Biophys. J.* **2002**, *83*, 633.
- (14) Frisch, M. J.; Trucks, G. W.; Schlegel, H. B.; Scuseria, G. E.; Robb, M. A.; Cheeseman, J. R.; Zakrzewski, V. G.; Montgomery, J. A.; Stratmann, R. E.; Burant, J. C.; Dapprich, S.; Millam, J. M.; Daniels, A. D.; Kudin, K. N.; Strain, M. C.; Farkas, O.; Tomasi, J.; Barone, V.; Cossi, M.; Cammi, R.; Mennucci, B.; Pomelli, C.; Adamo, C.; Clifford, S.; Ochterski, J.; Petersson, G. A.; Ayala, P. Y.; Cui, Q.; Morokuma, K.; Malick, D. K.; Rabuck, A. D.; Raghavachari, K.; Foresman, J. B.; Cioslowski, J.; Ortiz, J. V.; Stefanov, B. B.; Liu, G.; Liashenko, A.; Piskorz, P.; Komaromi, I.; Gomperts, R.; Martin, R. L.; Fox, D. J.; Keith, T. A.; Al-Laham, M. A.; Peng, C. Y.; Nanayakkara, A.; Gonzalez, C.; Challacombe, M.; Gill, P. M. W.; Johnson, B. G.; Chen, W.; Wong, M. W.; Andres, J. L.; Head-Gordon, M.; Replogle, E. S.; Pople, J. A. *GAUSSIAN 98*; Gaussian, Inc.: Pittsburgh, PA, 1998.
- (15) Becke, A. D. *J. Chem. Phys.* **1993**, *98*, 1372.
- (16) Becke, A. D. *J. Chem. Phys.* **1993**, *98*, 5648.
- (17) Stephens, P. J.; Devlin, F. J.; Chabalowski, C. F.; Frisch, M. J. *J. Phys. Chem.* **1994**, *98*, 11623.
- (18) Lee, C.; Yang, W.; Parr, R. G. *Phys. Rev. B* **1988**, *37*, 785.

Table 1. Calculated G^{K^+-A} , G^{Na^+-A} , G^{K^+} , and G^{Na^+} in Absorbance Units (1 AU = 627.51 kcal/mol; at 0 K Using B3LYP/6-311+G(2df,p)//B3LYP/6-31G(d) + ZPVE and at 298.15 K Using B3LYP/6-311+G(2df,p)//B3LYP/6-31G(d) + Thermal Correction)

energy	K ⁺ -A	Na ⁺ -A	K ⁺	Na ⁺
B3LYP/6-311+G(2df,p)	-2348.723 58	-1911.077 52	-599.761 05	-162.087 57
ZPVE	0.478 46	0.480 22		
$G(0K)$	-2348.245 12	-1910.597 31	-599.761 05	-162.087 57
thermal correction	0.402 57	0.406 92	0.001 42	0.001 42
$G(298.15K)$	-2348.321 01	-1910.670 60	-599.759 63	-162.086 15

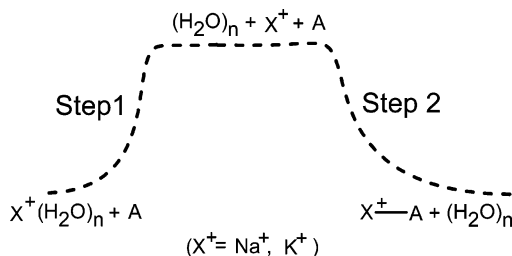


Figure 5. Schematic illustration of the stepwise mechanism for the loading of K⁺ and Na⁺ ions into the cavity end.

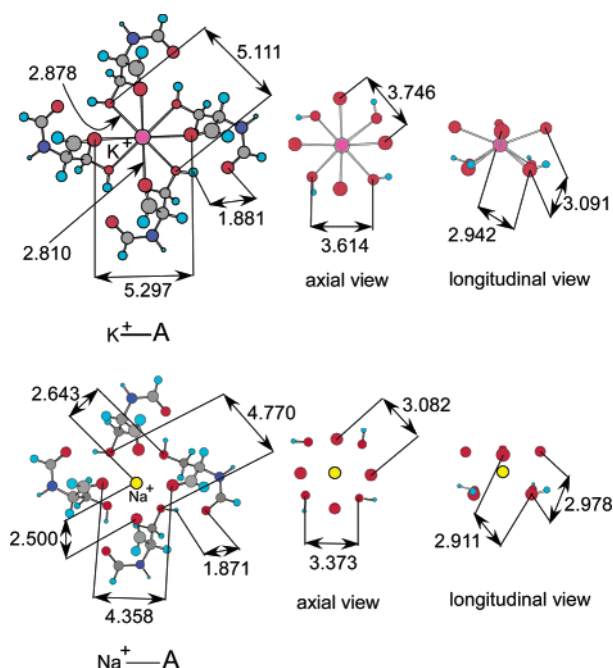


Figure 6. Optimized structures (K, pink; Na, yellow; O, red; C, grey; hydrogen, light blue) of K⁺-A and Na⁺-A at the B3LYP/6-31G(d) level.

that (5.297 Å) of the second oxygen ring of the carbonyl oxygens (Figure 6). The two layers of the oxygens that directly interact with the Na⁺ in Na⁺-A have the same conformation as in K⁺-A. However, the diameter (4.770 Å) of the first ring of the OH oxygens is larger than that (4.358 Å) of the second ring of the carbonyl oxygens (Figure 6). More detailed structural differences between K⁺-A and Na⁺-A are shown in Figure 6.

The formation free energies for K⁺-A and Na⁺-A complexes from K⁺ + A and Na⁺ + A are

$$\Delta G^{K^+-A} = G^{K^+-A} - (G^{K^+} + G^A)$$

$$\Delta G^{Na^+-A} = G^{Na^+-A} - (G^{Na^+} + G^A)$$

where G^{K^+-A} , G^{Na^+-A} , G^{K^+} , and G^{Na^+} are the free energies of K⁺-A, Na⁺-A, K⁺, and Na⁺. Thus, the affinity difference of

system A toward K⁺ with respect to Na⁺ is given by

$$\Delta\Delta G^{(K^+-A)-(Na^+-A)} = \Delta G^{K^+-A} - \Delta G^{Na^+-A} = (G^{K^+-A} - G^{Na^+-A}) - (G^{K^+} - G^{Na^+})$$

The calculated G^{K^+-A} , G^{Na^+-A} , G^{K^+} , and G^{Na^+} at 0 K are given in Table 1, where the $\Delta\Delta G^{(K^+-A)-(Na^+-A)}$ is calculated to be 16.1 kcal mol⁻¹ at 0 K and 14.5 kcal mol⁻¹ at 298.15 K, suggesting that the effect of temperature is relatively small. Thus, the K⁺ affinities at the cavity end of the filter (at 0 and 298.15 K, respectively), are approximately 16.1 and 14.5 kcal mol⁻¹ lower than their corresponding Na⁺ values. We thus concluded that the selectivity of the filter is not because of its stronger affinity for K⁺ ions. Clearly, other factors must help determine why the filter does not preferentially select Na⁺ at the intracellular cavity end.

Prior to being loaded into the selectivity filter, the K⁺ ion is hydrated within the cavity. Therefore, the energetics of the dehydration (step 1 in Figure 5) of K⁺ and Na⁺ may play an important role for the selectivity of the filter. At standard conditions, the solvation free energies for K⁺ and Na⁺ have been given as -80.6 and -98.2 kcal/mol by Noyes.¹⁹ More recent values for the solvation free energies of K⁺ and Na⁺ have been reported to be -84.1 and -101.3 kcal/mol, respectively.²⁰ Thus, the difference between K⁺ and Na⁺ solvation free energies is 17.2 kcal/mol. In vivo, the loading of K⁺ ions into the cavity end of the filter (i.e. the dehydration of the K⁺-water cluster and the binding of the dehydrated K⁺ ion to the hydroxyl oxygens of threonine or serine residues) should proceed as a concerted process. Hence, the free energy profiles for the loading of hydrated K⁺ and Na⁺ ions into the cavity end are more realistically described by those of a single loading step, shown as solid lines in Figure 7. Although Na⁺ ions have a 14.5 kcal mol⁻¹ larger affinity at the cavity end than K⁺ ions, it costs 17.2 kcal mol⁻¹ more energy to dehydrate a Na⁺ ion than it does for a K⁺ ion at the standard state. Overall, loading hydrated K⁺ ions into the cavity end is 2.7 kcal mol⁻¹ more favored than loading hydrated Na⁺ ions. Therefore, we suggest that the loading of hydrated K⁺ ions into the selectivity filter is preferentially favored.

The selectivity of the filter has also been probed by investigations of the free energy barriers for the conduction of K⁺ and Na⁺ ions across the filter. Aqvist and Luzhkov's molecular dynamics free energy perturbation calculations suggested that the switch of the two conduction states (S1)^{H₂O}(S2)^{K⁺}(S3)^{H₂O}-(S4)^{K⁺} and (S1)^{K⁺}(S2)^{H₂O}(S3)^{K⁺}(S4)^{H₂O} is 4.5 kcal/mol more selective for K⁺ than Na⁺.⁷ Berneche and Roux's molecular dynamics free energy simulation,⁹ in which the K⁺ ion at S1

(19) Noyes, R. M. *J. Am. Chem. Soc.* **1962**, *84*, 513.

(20) Tissandier, M. D.; Cowen, K. A.; Feng, W. Y.; Gundlach, E.; Cohen, M. H.; Earhart, A. D.; Tuttle, T. R.; Coe, J. V. *J. Phys. Chem. A* **1998**, *102*, 9308.

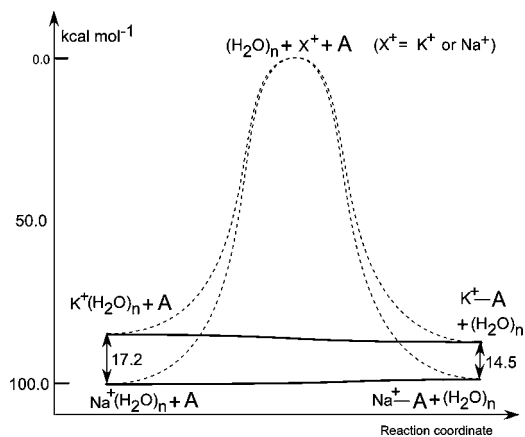


Figure 7. Schematic energy profiles for (a, in dashed lines) the stepwise mechanism and (b, in solid lines) the suggested concerted mechanism for the loading of K⁺ and Na⁺ into the cavity end.

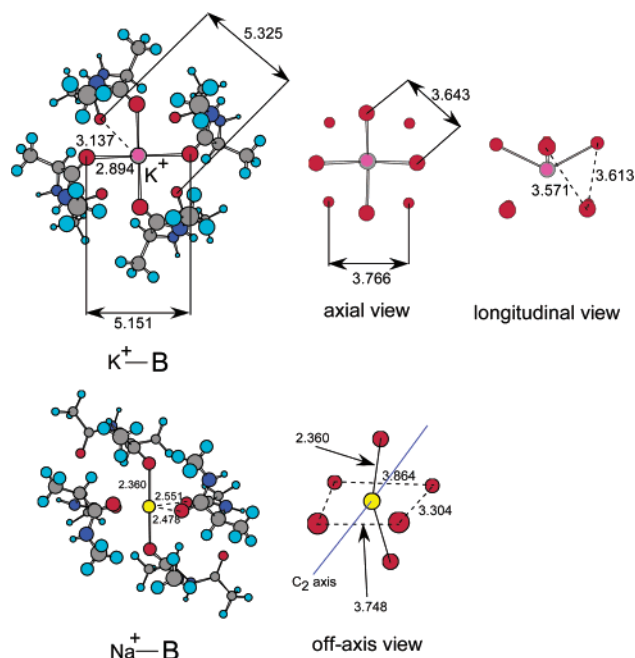


Figure 8. Optimized structures (K, pink; Na, yellow; O, red; C, grey; hydrogen, light blue) of K⁺-B and Na⁺-B.

and S2 is transformed into a Na⁺ ion, respectively, concluded that the excess free energy of S1 and S2 is 2.8 and 6.6 kcal mol⁻¹, suggesting that the existence of Na⁺ ions in the filter slows down the conduction of K⁺. However, our results suggest that there is selectivity for loading K⁺ ions even prior to the selectivity for their conduction.

Structural Preference of the Extracellular End of the Filter. To elucidate the structural preference of the extracellular end of the filter for the release of K⁺ ions, we have studied the energetics of releasing K⁺ and Na⁺ from their complexes with model system B (see Figure 4) of the extracellular end. The optimized structures of K⁺-B and Na⁺-B are shown in Figure 8.

The complex K⁺-B adopts a C₄ symmetric structure just as it is in the KscA K⁺ channel. It can be seen that the K⁺ ion in K⁺-B has a coordination number of eight, identical to that of the K⁺-(H₂O)₈ cluster.¹¹ However, we have found that Na⁺-B optimizes to a completely different structure with C₂ symmetry, in which the Na⁺ coordinates to only six carbonyl oxygen atoms

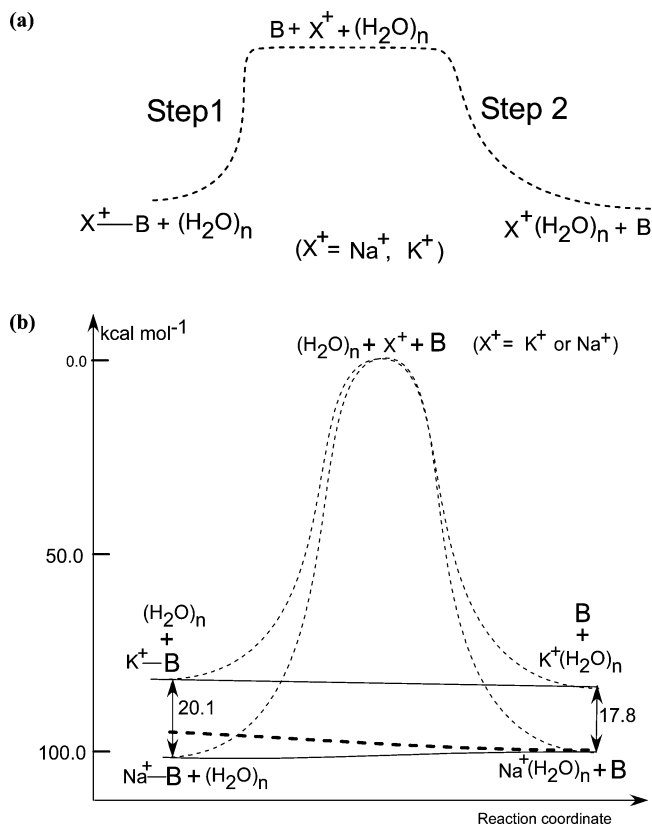


Figure 9. Schematic illustration of (a) the stepwise mechanism and (b) the energy profiles for the stepwise mechanism (thinner dashed lines), for the concerted single-step mechanism (solid lines) for the release of K⁺ and Na⁺ out of the extracellular end, and for the suggested real mechanism (thicker dashed line) for the release of Na⁺.

of the eight available. We conclude that the preferred coordination number of Na⁺ in the extracellular end of the K⁺ channel is actually six, whereas the designed coordination number within all K⁺ channels is eight.

Analogous to the loading of K⁺ ions into the cavity end, the release of K⁺ and Na⁺ ions from B is treated as a two-step process (Figure 9a), where the first step releases the ion from B and the second step is the hydration of the K⁺ or Na⁺ ion. For the first step, the difference between the K⁺ and Na⁺ affinities of model B is calculated by

$$\Delta\Delta G^{(K^+-B)-(Na^+-B)} = \Delta G^{K^+-B} - \Delta G^{Na^+-B} = (G^{K^+-B} - G^{Na^+-B}) - (G^{K^+} - G^{Na^+})$$

At 298.15 K, the $\Delta\Delta G^{(K^+-B)-(Na^+-B)}$ is calculated to be 20.1 kcal mol⁻¹. Since Na⁺ ions have a hydration free energy only 17.2 kcal mol⁻¹ lower than K⁺ ions, the release of K⁺ ions is 2.9 kcal mol⁻¹ more favored than the release of Na⁺ ions if the extracellular end of the filter were flexible enough to achieve the optimal coordination structures for both K⁺ and Na⁺ ions. However, the 20.1 kcal mol⁻¹ stronger Na⁺ affinity at the extracellular end would lead to the preferential back-loading of Na⁺ ions into the extracellular end and therefore inhibit K⁺ ion departure. However, structural considerations preclude this. The cooperation of the five specific amino acid residues (as shown in Figure 3) that make up the four identical units of the selectivity filter is able to maintain the desired balance between their rigidity and dynamic flexibility. Due to the large size of nonpolar Val and Tyr side chains, we observe that one of their

functions is to minimize the flexibility, thereby maximizing the rigidity of the five residues for each single unit of the filter. Thus, the extracellular end of the filter preferentially provides an eight-carbonyl-oxygen-coordinating environment for K^+ ions rather than the optimal six-carbonyl-oxygen-coordinating environment for Na^+ ions and therefore can avoid unwanted inhibition of the channel by Na^+ ion insertion. The actual difference between the K^+ and Na^+ affinities of the extracellular end should be larger than the difference between the K^+ and Na^+ affinities of the cavity end ($14.5 \text{ kcal mol}^{-1}$) and smaller than the difference ($17.2 \text{ kcal mol}^{-1}$) of the hydration free energies of K^+ and Na^+ ions, so that the conduction of K^+ ions is direction specific from inside to outside of the cell. In Figure 9b the thicker dashed line schematically shows a possible free energy profile for the release of Na^+ ions from the true (adequately rigid) extracellular end of the filter. Clearly, the difference of the optimized structures of Na^+-B and K^+-B provides fundamental theoretical evidence that the K^+ channel is specifically optimized for the conduction and releasing of K^+ ions.

Conclusions

The chemical basis for the selectivity filter of the K^+ channel has been investigated with the B3LYP density functional theory method. We have focused on elucidation of the energetics of loading and releasing Na^+ and K^+ ions in to and out of the selectivity filter.

The optimized structures of the complexes of K^+-A and Na^+-A suggest that the 4-fold symmetric conformation of the cavity end of the selectivity filter is structurally preferred for

both Na^+ and K^+ ions. Specifically, the eight coordination of four threonine- or serine-hydroxyl groups and four valine-carbonyl oxygens are optimal to both K^+ and Na^+ ions. However, the loading of K^+ ions into the cavity end of the selectivity filter from the solution phase is approximately $2.7 \text{ kcal mol}^{-1}$ more favored than the loading of Na^+ ions. We conclude that the selectivity of the filter begins with the loading of K^+ ions into the filter.

The optimized structures of the K^+-B and Na^+-B complexes at the extracellular end of the selectivity filter suggest that K^+ ions prefer the "natural design" of an eight-carbonyl-oxygen-coordinated environment in the selectivity filter, whereas Na^+ ions prefer coordination to six of the carbonyl oxygens in the protein backbone. On the basis of these structural differences, it can be concluded that the rigid 4-fold symmetry of the K^+ channel is solely optimized for K^+ ions, not for Na^+ ions.

A major component of the chemical-physical basis for the selectivity for K^+ over Na^+ of the selectivity filter lies in the differences between the solvation free energies and the K^+ and Na^+ affinities of the cavity end. Further study to extend the above conclusion to the entire series of ions Li^+ , Na^+ , K^+ , Rb^+ , and Cs^+ is being undertaken.

Acknowledgment. D.F.W. acknowledges support of a Canada Research Chair in Neuroscience.

Supporting Information Available: Archive entries of the B3LYP/6-31G(d) optimized structures (PDF). This material is available free of charge via the Internet at <http://pub.acs.org>.

JA0367290